

Probing the Interaction of Trans-resveratrol with Bovine Serum Albumin: A Fluorescence Quenching Study with Tachiya Model

J. B. Xiao · X. Q. Chen · X. Y. Jiang · M. Hilczer · M. Tachiya

Received: 21 June 2007 / Accepted: 7 February 2008 / Published online: 20 March 2008
© Springer Science + Business Media, LLC 2008

Abstract The interaction of trans-resveratrol (TRES) and bovine serum albumin (BSA) was investigated using fluorescence spectroscopy (FS) with Tachiya model. The binding number maximum of TRES was determined to be 8.86 at 293.15 K, 23.42 at 303.15 K and 33.94 at 313.15 K and the binding mechanism analyzed in detail. The apparent binding constants (K_a) between TRES and BSA were 5.02×10^4 (293.15 K), 8.89×10^4 (303.15 K) and 1.60×10^5 L mol⁻¹ (313.15 K), and the binding distances (r) between TRES and BSA were 2.44, 3.01, and 3.38 nm at 293.15, 303.15, and 313.15 K, respectively. The addition of TRES to BSA solution leads to the enhancement in RLS intensity, exhibiting the formation of the aggregate in solution. The negative entropy change and enthalpy change

indicated that the interaction of TRES and BSA was driven mainly by van der Waals interactions and hydrogen bonds. The process of binding was a spontaneous process in which Gibbs free energy change was negative.

Keywords Bovine serum albumin · Fluorescence spectroscopy · Interaction · Trans-resveratrol · Tachiya model

Introduction

The interaction between bio-macromolecules and drugs has attracted great interest among researchers since several decades [1–3]. Among bio-macromolecules, serum albumin is the major soluble protein constituent of circulatory system and has many physiological functions. The most outstanding function of serum albumin is that it serves as a depot protein and a transport protein for many exogenous compounds [4–5]. The drug–protein interaction may result in the formation of a stable protein–drug complex, which has important effect on the distribution, free concentration and the metabolism of drug in the blood stream. Thus, the drug–albumin complex may be considered as a model for gaining fundamental insights into drug–protein interactions. Therefore, studies on the binding of drug with protein will facilitate interpretation of the metabolism and transporting process of drug, and will help to explain the relationship between structures and functions of protein. In this regard, bovine serum albumin (BSA) has been studied extensively, partly because of its structural homology with human serum albumin (HSA) [6–10].

Trans-resveratrol (TRES), trans-3,5,4-trihydroxy stilbene (Fig. 1), is one of the major stilbene phytoalexins found in various families of plants, but grapes, peanuts, and their

J. B. Xiao · X. Q. Chen (✉) · X. Y. Jiang
College of Chemistry and Chemical Engineering,
Central South University,
Changsha 410083, People's Republic of China
e-mail: xqchencsu@yahoo.com

J. B. Xiao
Department of Nutrition, Faculty of Health and Welfare,
Okayama Prefectural University,
Kuboki 111,
Soja, Okayama 719-1197, Japan

M. Hilczer
Institute of Applied Radiation Chemistry,
Technical University of Lodz,
Wroblewskeigo 15,
93-590 Lodz, Poland

M. Tachiya (✉)
National Institute of Advanced Industrial
Science and Technology (AIST),
AIST Central 5,
Tsukuba, Ibaraki 305-8565, Japan
e-mail: m.tachiya@aist.go.jp

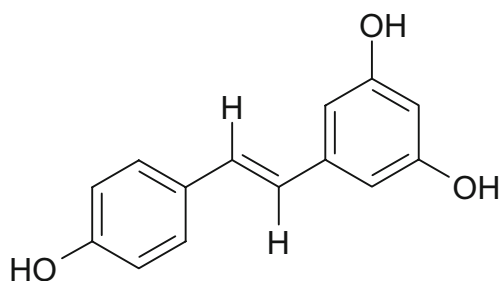


Fig. 1 Structure of TRES

products are considered the most important dietary sources of the TRES [11]. Several epidemiological studies have shown that red wine consumption is inversely related to cardiovascular disease and TRES has been studied as the potential protective component [12]. Research over the past several decades has revealed that TRES exerts multifarious biological effects, including potent antioxidant, anti-inflammatory, antiplatelet, and antiproliferative effects [13–17].

Fluorescence spectroscopy is an appropriate method to determine the interaction between the small molecule ligand and bio-macromolecule. By means of measurement and analysis of the emission peak, the transfer efficiency of energy, the lifetime, and fluorescence polarization, etc., much information may be obtained concerning the structural changes and the microenvironment surrounding the fluorophore in the macromolecule.

To gain some insights into the medicinal action of TRES, the interactions between TRES and BSA were investigated by means of fluorescence spectroscopy with Tachiya model. Some important information such as the apparent binding constants and binding sites values were obtained. And the results were compared with that of modified Stern–Volmer equation.

Model

Adsorption and desorption of a molecule to and from BSA is given by



where B_n stands for BSA with n quenchers. If the number of binding sites in BSA is m , it is reasonable to assume that the rate constant for process 1 is given by

$$\text{Adsorption rate constant} = \begin{cases} 1 - \frac{n}{m} k_1 & \text{for } n \leq m \\ 0 & \text{for } n > m \end{cases} \quad (3)$$

The rate constant for process 2 is given by

$$\text{desorption rate constant} = nk_2 \quad (4)$$

Here, k_1 is the absorption rate constant and k_2 is the desorption rate constant. The number of binding sites (m) is different from the number of molecules (n) actually bound to the sites. The number of molecules bound to the binding sites follows a binomial distribution, if the number of binding sites is fixed [18].

$$Q_n = {}_m C_n \left(\frac{n_{av}}{m}\right)^n \left(1 - \frac{n_{av}}{m}\right)^{m-n} \quad (5)$$

Here n_{av} is the average number of bound quenchers in a biomolecule and is given by [1]

$$n_{av} = mK \frac{[Q_{aq}]}{m + K[Q_{aq}]} \quad (6)$$

where $[Q_{aq}]$ stands for the concentration in aqueous solution and $K = k_1/k_2$. If we denote the concentration of BSA by $[M]$, the total concentration $[Q]$ of quenchers added in solution is given by,

$$[Q] = n_{av}[M] + [Q_{aq}] \quad (7)$$

Eliminating $[Q_{aq}]$ from Eqs. 6 and 7, we have

$$n_{av} = \frac{1}{2} \left[\frac{[Q]}{[M]} + m + \frac{m}{K}[M] - \sqrt{\left(\frac{[Q]}{[M]} + m + \frac{m}{K}[M]\right)^2 - 4m \frac{[Q]}{[M]}} \right] \quad (8)$$

The rate constant for Foerster energy transfer from BSA to a quencher is given by

$$k_e = \tau^{-1} \left(\frac{R_0}{r}\right)^6 \quad (9)$$

where τ is the lifetime of BSA in the absence of quencher, r is the distance between BSA to the quencher, and R_0 is the Foerster distance. If a biomolecule has n bound quenchers at the same distance r from BSA, the fluorescence intensity is reduced to

$$F = \frac{1}{1 + n \left(\frac{R_0}{r}\right)^6} \quad (10)$$

compared to the case of no bound quencher. Therefore, the ratio of the fluorescence intensities in the presence and absence of added quenchers is given by

$$\frac{F}{F_0} = \sum_{n=0}^m \frac{Q_n}{1 + n \left(\frac{R_0}{r}\right)^6} = \sum_{n=0}^m \frac{{}_m C_n \left(\frac{n_{av}}{m}\right)^n \left(1 - \frac{n_{av}}{m}\right)^{m-n}}{1 + n \left(\frac{R_0}{r}\right)^6} \quad (11)$$

where n_{av} is given by Eq. 8. In Eq. 11 combined with Eq. 8 the values of $[M]$, $[Q]$ and F/F_0 are experimentally known or obtainable. The unknown parameters are m , K and r . They are determined by fitting Eq. 11 to the experimentally obtained dependence of F/F_0 on $[Q]$ and $[M]$.

The following limiting forms of Eq. 11 may be useful when one fits it to the observed dependence of F/F_0 on $[Q]$.

At a fixed value of $[M]$, F/F_0 in general decreases with increasing $[Q]$. However, it saturates at sufficiently high $[Q]$ because once all binding sites in BSA are occupied by quenchers, further increase in $[Q]$ does not increase the number of bound quenchers. At saturation the distribution of the number of bound quenchers is given by

$$Q_n = \delta(n - m) \tag{12}$$

Therefore, the saturated fluorescence intensity is given by

$$\left(\frac{F}{F_0}\right)_{\text{saturation}} = \frac{1}{1 + m\left(\frac{R_0}{r}\right)^6} \tag{13}$$

At sufficiently low $[Q]$ the average number of bound quenchers in a biomolecule is small and calculated from Eq. 8 as

$$n_{\text{av}} = \frac{K[Q]}{K[M] + 1} \tag{14}$$

In this case the distribution the number of bound quenchers is approximated as

$$Q_n = 1 - n_{\text{av}} \quad \text{for } n = 0 \\ = n_{\text{av}} \quad \text{for } n = 1 \tag{15}$$

Therefore, the fluorescence intensity is given by

$$\frac{F}{F_0} = 1 - n_{\text{av}} \frac{\left(\frac{R_0}{r}\right)^6}{1 + \left(\frac{R_0}{r}\right)^6} = 1 - \frac{\left(\frac{R_0}{r}\right)^6}{1 + \left(\frac{R_0}{r}\right)^6} \frac{K[Q]}{K[M] + 1} \tag{16}$$

where n_{av} is given by Eq. 14.

Experimental

Apparatus

Fluorescence and resonance light scattering spectra were recorded on a JASCO FP-6500 spectrofluorometer equipped with a thermostated cell compartment using quartz cuvettes (1.0 cm) (Tokyo, Japan). The ultraviolet-visible (UV-vis) spectra were recorded on a UV-2450 spectrophotometer using quartz cuvettes (1.0 cm; Shimadzu, Japan). The pH measurements were carried out on a PHS-3C Exact Digital pH meter equipped with Phonix Ag-AgCl reference electrode (Cole-Paemer Instrument), which was calibrated with standard pH buffer solutions.

Reagents

TRES was obtained commercially from the National Institute for the Control of Pharmaceutical and Biological Products (Beijing, China). A working solution of TRES

($0.5 \times 10^{-3} \text{ mol L}^{-1}$) was prepared by dissolving TRES in methanol–water solution (1:1, v/v). Bovine serum albumin (fraction V) was purchased from Sigma Co. (St. Louis, MO, USA). The working solution of BSA ($1.0 \times 10^{-5} \text{ mol L}^{-1}$) in the doubly distilled water was prepared and stored in refrigerator prior to use. Tris–HCl buffer (0.20 mol L^{-1} , pH 7.4) containing 0.10 mol L^{-1} NaCl was selected to keep the pH value and maintain the ionic strength of the solution. All other reagents and solvents were of analytical reagent grade and used without further purification unless otherwise noted. All aqueous solutions were prepared using newly double-distilled water.

Fluorescence and ultraviolet spectra

Appropriate quantities of $0.5 \times 10^{-3} \text{ mol L}^{-1}$ TRES solution were transferred to a 10 mL flask, and then 0.5 or 1.0 mL of BSA solution was added and diluted to 10 mL with water. The resultant mixture was subsequently ultrasonicated for 5 min and incubated at 293.15, 303.15, or 313.15 K for 2 h. The solution was scanned on the fluorophotometer with the range of 290–500 nm. The fluorescent intensity at 340 nm was determined under the excitation at wavelength of 280 nm. The operations were carried out at fixed temperature (293.15, 303.15, and 313.15 K).

The UV spectra were obtained by scanning the solution on the spectrophotometer with the wavelength range of 220–400 nm. The operations were carried out at room temperature.

Resonance light scattering spectra

An appropriate aliquot of TRES working solution was added to 1.0 mL BSA working solution, and diluted to 10 mL with water. RLS spectra were obtained by synchronous scanning with the wavelength range of 250–750 nm on the spectrofluorophotometer. The operations were carried out at room temperature.

Results and discussions

Characteristics of the fluorescence spectra

The fluorescence spectra of BSA in the presence of different concentrations of TRES were shown in Figs. 2 and 3. With the increasing concentration of TRES, the fluorescence intensity of BSA decreased remarkably. The high concentration of TRES ($5.00 \times 10^{-5} \text{ mol L}^{-1}$) may quench completely BSA fluorescence and only the fluorescence of TRES was observed (Fig. 3h). There was significant λ_{em} red shift with the addition of TRES, indicating that interactions

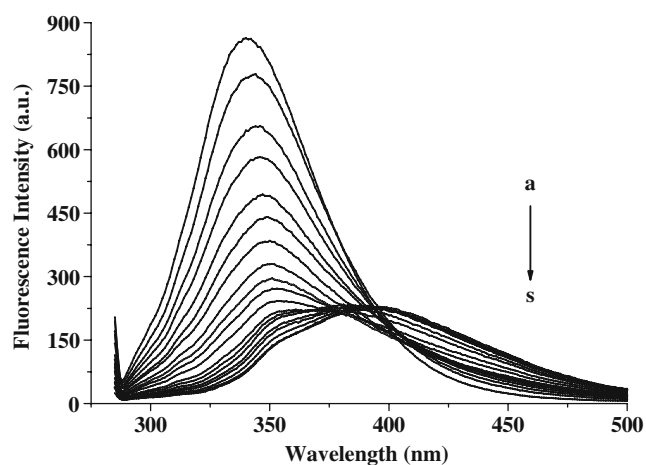


Fig. 2 The quenching effect of TRES on BSA fluorescence intensity. $\lambda_{\text{ex}}=280$ nm, (a–s) BSA, 0.50×10^{-6} mol L $^{-1}$: 0.00, 0.25, 0.50, 0.75, 1.00, 1.25, 1.50, 1.75, 2.00, 2.25, 2.50, 2.75, 3.00, 3.25, 3.50, 3.75, 4.00, 4.25, 4.50 ($\times 10^{-5}$ mol L $^{-1}$) of TRES

between TRES and BSA occurred and TRES–BSA complex may form.

The critical energy-transfer distance between the drug and the amino acid residues of BSA

According to the Förster non-radiation energy transfer theory [19, 20], the energy-transfer effect is related not only to the distance between the acceptor and donor, but also to the critical energy-transfer distance (R_0).

$$R_0^6 = 8.8 \times 10^{-25} K^2 N^4 \Phi J \quad (17)$$

where K^2 is the spatial orientation factor of the dipole, N the refractive index of the medium, Φ the fluorescence quantum yield of the donor, and J the overlap integral of the

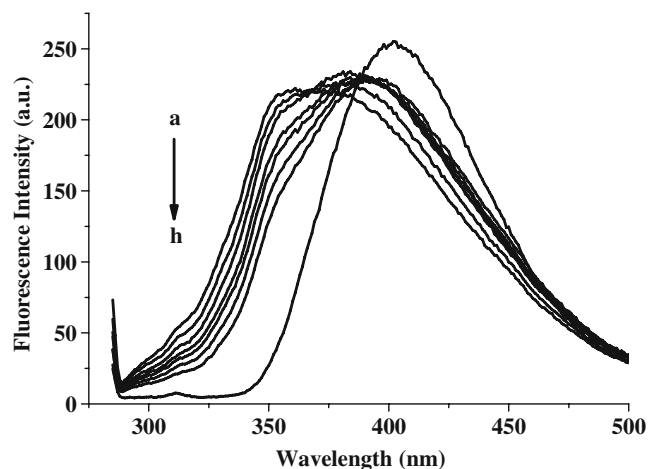


Fig. 3 The fluorescence spectra of TRES–BSA systems and TRES. $\lambda_{\text{ex}}=280$ nm, (a–h) BSA, 0.0×10^{-5} mol L $^{-1}$: 2.75, 3.00, 3.25, 3.50, 3.75, 4.00, 4.25, and 5.00 ($\times 10^{-5}$ mol L $^{-1}$) of TRES

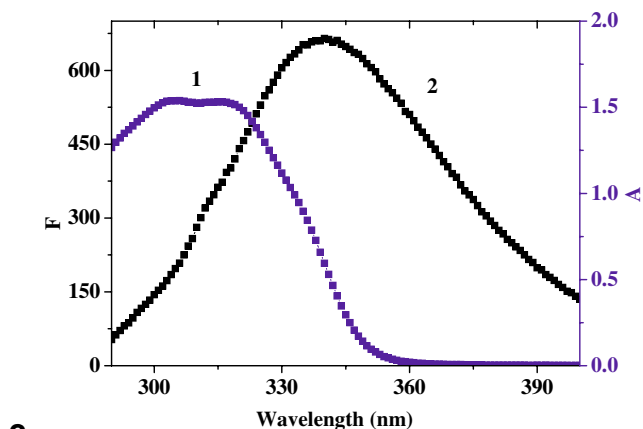
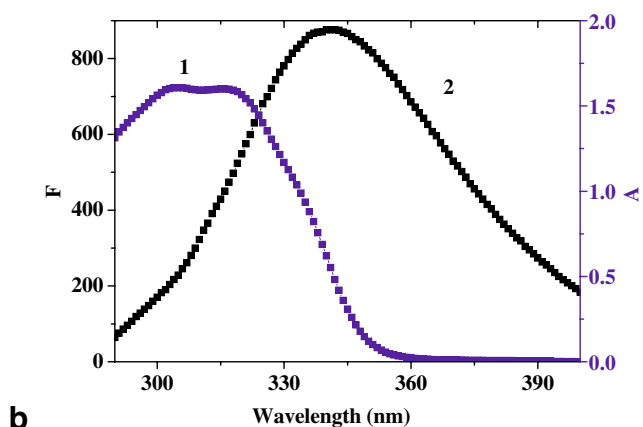
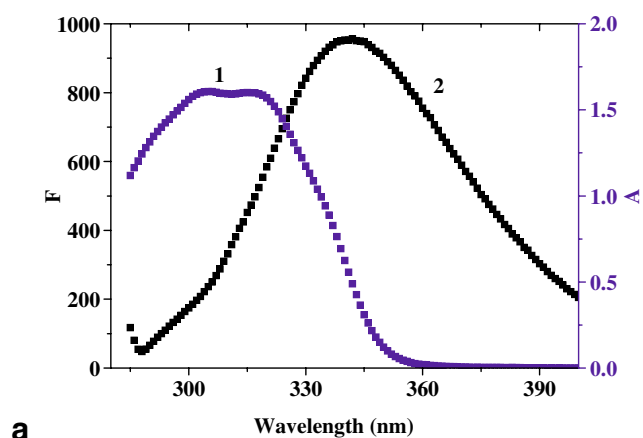


Fig. 4 Overlap spectra of TRES UV absorption spectra (1) and BSA's fluorescence emission spectra (2) at 293.15 (a), 303.15 (b), and 313.15 K (c): $C_{\text{BSA}}=1.0 \times 10^{-5}$ mol L $^{-1}$, $C_{\text{TRES}}=4.5 \times 10^{-5}$ mol L $^{-1}$

fluorescence emission spectrum of the donor and the absorption spectrum of the acceptor [20]. Therefore,

$$J = \frac{\int_0^\infty F(\lambda)\varepsilon(\lambda)\lambda^4 d\lambda}{\int_0^\infty F(\lambda)d\lambda} \quad (18)$$

Here $F(\lambda)$ is the fluorescence intensity of the fluorescence donor at wavelength λ and $\varepsilon(\lambda)$ the molar absorptivity of the acceptor at wavelength λ .

Table 1 The overlap integrals and the critical distance^a

Temperature (K)	J (cm ³ l mol ⁻¹)	R_0 (nm)
293.15	1.82×10^{-14}	2.71
303.15	1.96×10^{-14}	2.74
313.15	1.88×10^{-14}	2.72

^a R_0 was calculated from the Eq. 5 when $K^2 = 2/3$, $N = 1.336$ and $\Phi = 0.118$ [3]

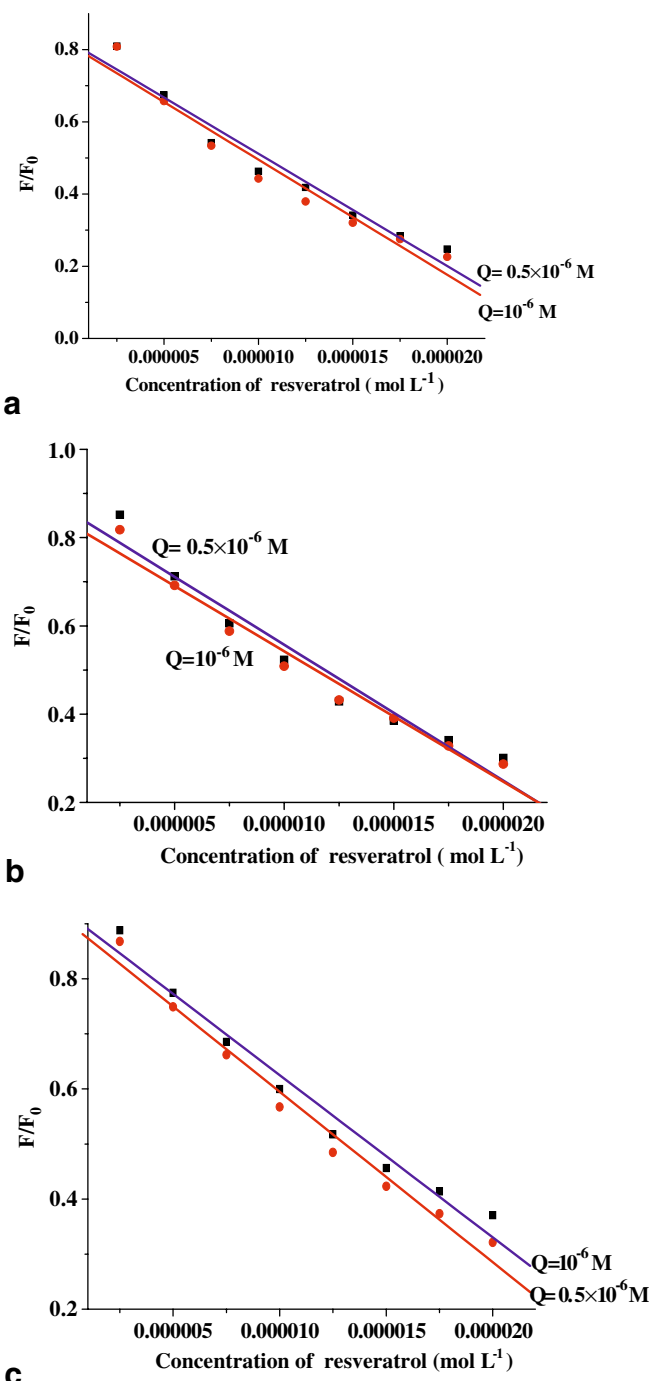


Fig. 5 The F/F_0 vs $[Q]$ curves at 293.15 (a), 303.15 (b), and 313.15 K (c)

The overlap of the absorption spectrum of TRES and the fluorescence emission spectrum of BSA at different temperature were shown in Fig. 4. The overlap integrals and the critical distance in different temperature were shown in Table 1. The critical energy-transfer distance (R_0) was hardly changed with the increasing temperature. And the critical energy-transfer distance (R_0) was a constant when the measuring parameters of fluorescence intensity were different from each other, such as excitation slits, emission slits, and volt.

Quenching constants and binding distance

Fluorescence quenching could proceed via different mechanisms, usually classified as dynamic quenching and static quenching. Higher temperatures will result in faster diffusion and hence larger amounts of collisional quenching and higher temperatures will typically result in the dissociation of weakly bound complexes and hence smaller amounts of static quenching. For the dynamic quenching, the mechanism can be described by the Tachiya model [18].

According to my Eq. 16, F/F_0 should be proportional to $[Q]$ at sufficiently low $[Q]$, and the proportionality coefficient depends on K , r and $[M]$. Therefore, the values of K and r can be determined by measuring the F/F_0 vs $[Q]$ curves for two different values of $[M]$ (Fig. 5). At sufficiently high $[Q]$ the value of F/F_0 should saturate to the value given by my Eq. 13. The value of m was obtained according to Eq. 13.

The temperature-dependent fluorescence quenching of BSA by TRES was then carried out. The F/F_0 vs $[Q]$ curves at different temperatures were shown in Fig. 5. From the experimental data, the corresponding quenching constants for the interaction between TRES and BSA were $K = 5.02 \times 10^4$ L mol⁻¹ (293.15 K), $K = 8.89 \times 10^4$ L mol⁻¹ (303.15 K) and $K = 1.60 \times 10^5$ L mol⁻¹ (313.15 K), respectively. The K increased with increasing temperature (Table 2). The binding number maximum of TRES was determined to be 8.86 at 293.15 K, 23.42 at 303.15 K and 33.94 at 313.15 K.

The basic principles like excited state reactions, molecular rearrangements, energy transfer, ground state complex formation, and collisional quenching involves in molecular interaction, which can result in quenching. Quenching can occur by different mechanisms like dynamic quenching and static quenching. The mechanism can be distinguished from

Table 2 The binding parameters for the system of TRES–BSA by Tachiya model

Temperature (K)	Binding constant (l mol ⁻¹)	Binding site	r (nm)
293.15	5.02×10^4	8.86	2.44
303.15	8.89×10^4	23.42	3.01
313.15	1.60×10^5	33.94	3.38

Table 3 The binding parameters for the system of TRES–BSA by modified Stern–Volmer equation

Temperature (K)	Binding constant (l mol^{-1})	Binding site	r (nm)
293.15	$1.27 \pm 0.05 \times 10^5$	1.22 ± 0.02	3.47
303.15	$1.03 \pm 0.02 \times 10^5$	1.18 ± 0.05	3.73
313.15	$8.22 \pm 0.04 \times 10^4$	1.25 ± 0.01	3.99

the differing dependence on temperature and viscosity on the Stern–Volmer constant (K_{SV}) values. Dynamic quenching depends upon diffusion. Since higher temperatures results larger diffusion coefficients, the bimolecular quenching constants are expected to increase with increasing temperature (Table 2). In contrast, increased temperature is likely to result in decreased stability of complexes, and thus lower values of the static quenching constants.

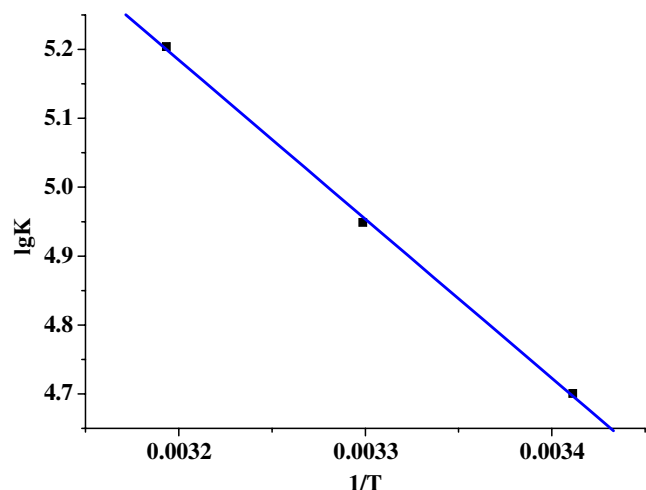
Binding constant and binding sites by modified Stern–Volmer equation

For static quenching, the relationship between fluorescence quenching intensity and the concentration of quenchers can be described by the binding constant formula [21]:

$$\lg \frac{F_0 - F}{F} = m \lg K_a + m \lg \left([Q] - [M] \frac{F_0 - F}{F} \right) \quad (19)$$

where K_a is the binding constant, and m is the number of binding sites per BSA. After the fluorescence quenching intensities on BSA at 340 nm were measured, the double-logarithm algorithm was assessed by Eq. 19.

According to the Förster non-radiation energy transfer theory, the energy-transfer effect is related not only to the distance between the acceptor and donor, but also to the critical energy-transfer distance (R_0).

**Fig. 6** $\lg K$ vs. $1/T$ for TRES–BSA system**Table 4** The thermodynamic parameters of TRES–BSA binding procedure

Temperature ($^{\circ}\text{C}$)	ΔH (kJ mol^{-1})	ΔG (kJ mol^{-1})	ΔS ($\text{J mol}^{-1} \text{K}^{-1}$)
20		-6.86	
30	-12.58	-6.76	-19.20
40		-6.57	

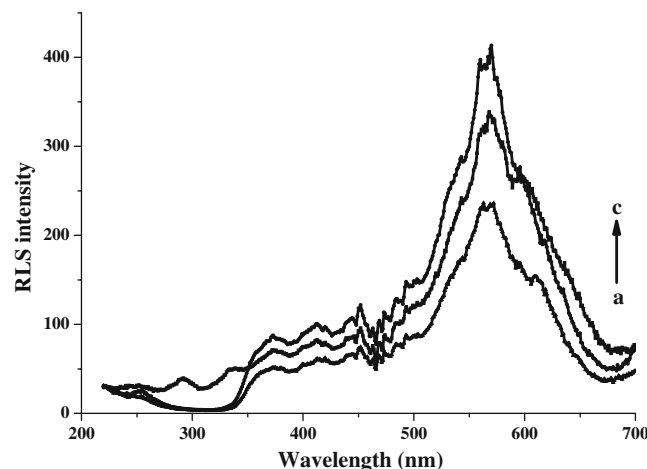
$$E = \frac{R_0^6}{(R_0^6 + r^6)} \quad (20)$$

$$E = 1 - \frac{F}{F_0} \quad (21)$$

where E is the energy transfer efficiency, R_0 is the critical distance when the transfer efficiency is 50%, and r is the binding distance between donor and acceptor.

Table 3 gave the corresponding calculated results. The apparent binding constants (K_a) between TRES and BSA were $1.27 \pm 0.05 \times 10^5$ (293.15 K), $1.03 \pm 0.02 \times 10^5$ (303.15 K) and $8.22 \pm 0.04 \times 10^4$ (313.15 K). The binding constants from the Stern–Volmer equation decreased with the increasing temperature (Table 3). However, the binding constants from the Tachiya model increased with the increasing temperature (Table 2).

The data clearly showed that the binding sites by Stern–Volmer equation on BSA for TRES obtained by the Stern–Volmer equation were independent of temperature from 293.15 to 313.15 K. As shown in Table 2 and 3, the binding constants and binding sites obtained by modified Stern–Volmer equation and Tachiya model were different from each other. For Stern–Volmer equation, difference between the number of binding sites (m) and the number of molecules (n) actually bound to the sites was not taken into account. The

**Fig. 7** RLS spectra of $0.5 \times 10^{-4} \text{ mol L}^{-1}$ TRES (a), $1.0 \times 10^{-6} \text{ mol L}^{-1}$ BSA (b), and $1.0 \times 10^{-4} \text{ mol L}^{-1}$ TRES and $1.0 \times 10^{-6} \text{ mol L}^{-1}$ BSA (c)

binding distances between TRES and BSA by modified Stern–Volmer equation were almost the same as that of Tachiya model and increased with the increasing temperature.

Thermodynamic parameters and nature of the binding forces

The interaction forces between drug and biomolecule may involve hydrophobic forces, electrostatic interactions, van der Waals interactions, hydrogen bonds, etc. According to the data of enthalpy change (ΔH) and entropy change (ΔS), the model of interaction between drug and biomolecule can be concluded [22]: (1) $\Delta H > 0$ and $\Delta S > 0$, hydrophobic forces; (2) $\Delta H < 0$ and $\Delta S < 0$, van der Waals interactions and hydrogen bonds; (3) $\Delta H < 0$ and $\Delta S > 0$, electrostatic interactions. In order to elucidate the interaction of TRES with BSA, we calculated the thermodynamic parameters from the Van't Hoff equation:

$$\ln K = -\frac{\Delta H}{RT} + \frac{\Delta S}{R} \quad (22)$$

The free energy change (ΔG) can be estimated from the following equation, based on the binding constants at different temperatures:

$$\Delta G = \Delta H - T \Delta S \quad (23)$$

Figure 6, by fitting the data of Table 2, it shows that assumption of near constant ΔH is justified. Table 4 shows the values of ΔH and ΔS obtained for the binding site from the slopes and ordinates at the origin of the fitted lines. The binding process is spontaneous is evidenced by the negative values of free energy (ΔG ; Table 4).

The thermodynamic parameters for the interaction of TRES with BSA are shown in Table 4. The negative sign for ΔG means that the interaction process is spontaneous. The negative ΔH and ΔS values indicated that van der Waals interactions and hydrogen bonds may play a major role in the binding between TRES and BSA [20]. The characteristic of albumin to allow a variety of ligands to bind to it is amazing. Albumin is the principal carrier of drugs that are otherwise insoluble in the circulating plasma. Van der Waal's interactions and hydrogen bonds play major role in the protein ligand interaction [23]. Hydrogen bonds are specific and directed, which may be best identified through their negative enthalpy of complex formation.

Characteristics of the RLS spectra

The RLS spectra of TRES–BSA in Tris–HCl buffer solution (0.020 mol L⁻¹) were shown in Fig. 7. It can be seen that the RLS intensity of free TRES is weaker than that of TRES–BSA system (Fig. 7c) in the range of 400–700 nm. Upon addition of trace amount of TRES to BSA solution, a remarkably enhanced RLS with a maximum

peak at 570.0 nm and a secondary one at 452.0 nm was observed (Fig. 7b–c).

Resonance light scattering (RLS), an elastic scattering, occurs when an incident beam is close to an absorption band. Pasternack et al. first established the RLS technique to study the bio-macromolecules on an ordinary fluorescence spectrometer. RLS is a sensitive and selective technique for monitoring molecular assemblies. RLS have attracted great interest among researchers [24–28]. The production of RLS is correlated with the formation of certain aggregate and the RLS intensity is dominated primarily by the particle dimension of the formed aggregate in solution. Bearing these points in mind, it is inferred from the results that the added BSA may interact with TRES in solution, forming a new TRES–BSA complex that could be expected to be an aggregate. The newly formed TRES–BSA complex may be ascribed to the higher electrostatic attraction between TRES and BSA. The size of TRES–BSA particles may be larger than that of BSA, and thus the increased light-scattering signal occurred under the given conditions. Moreover, the dimension of the resultant TRES–BSA particles may be much less than the incident wavelength, and thus the enhanced light-scattering signal occurs under the given conditions.

Conclusion

The interaction of TRES and bovine serum albumin (BSA) was investigated using fluorescence spectroscopy (FS) with Tachiya model. The binding number maximum of TRES was determined to be 8.86 at 293.15 K, 23.42 at 303.15 K and 33.94 at 313.15 K and the binding mechanism analyzed in detail. The apparent binding constants (K_a) between TRES and BSA were 5.02×10^4 (293.15 K), 8.89×10^4 (303.15 K) and 1.60×10^5 L mol⁻¹ (313.15 K), and the binding distances (r) between TRES and BSA were 2.44, 3.01, and 3.38 at 293.15, 303.15, and 313.15 K, respectively. The negative entropy change and enthalpy change indicated that the interaction of TRES and BSA was driven mainly by van der Waals interactions and hydrogen bonds. The process of binding was a spontaneous process in which Gibbs free energy change was negative.

Acknowledgments The authors are grateful for financial supported by National Natural Science Foundation of China (grant No. 20776162 and 20775092).

References

- Xiang GH, Tong CL, Lin HZ (2007) Nitroaniline Isomers Interaction with Bovine Serum Albumin and Toxicological Implications. *J Fluoresc* 17:512–521

2. Soares S, Mateus N, Freitas V (2007) Interaction of Different Polyphenols with Bovine Serum Albumin (BSA) and Human Salivary α -Amylase (HSA) by Fluorescence Quenching. *J Agric Food Chem* 55:6726–6735
3. Xiao JB, Shi J, Cao H, Wu SD, Ren FL, Xu M (2007) Analysis of binding interaction between puerarin and bovine serum albumin by multi-spectroscopic method. *J Pharmaceut Biomed* 45:609–615
4. Ran D, Wu X, Zheng J, Yang J, Zhou H, Zhang M, Tang Y (2007) Study on the interaction between florasulam and bovine serum albumin. *J Fluoresc* 17:721–726
5. Cui FL, Wang JL, Cui YR, Li JP (2006) Fluorescent investigation of the interactions between N-(p-chlorophenyl)-N'-(1-naphthyl) thiourea and serum albumin: synchronous fluorescence determination of serum albumin. *Anal Chim Acta* 571:175–183
6. Shang L, Jiang X, Dong S (2006) In vitro study on the binding of neutral red to bovine serum albumin by molecular spectroscopy. *J Photochem Photobiol A* 184:93–97
7. Bose B, Dube A (2006) Interaction of Chlorin p6 with bovine serum albumin and photodynamic oxidation of protein. *J Photochem Photobiol B* 85:49–55
8. Zhou N, Liang YZ, Wang P (2007) 18b-Glycyrrhetic acid interaction with bovine serum albumin. *J Photochem Photobiol A* 185:271–276
9. Hu YJ, Liu Y, Zhao RM, Dong JX, Qu SS (2006) Spectroscopic studies on the interaction between methylene blue and bovine serum albumin. *J Photochem Photobiol A* 179:324–329
10. Wang YP, Wei YL, Dong C (2006) Study on the interaction of 3,3-bis(4-hydroxy-1-naphthyl)-phthalide with bovine serum albumin by fluorescence spectroscopy. *J Photochem Photobiol A* 177:6–11
11. Cao H, Xiao JB, Xu M (2006) Evaluation of new selective molecularly imprinted polymers for the extraction of resveratrol from *Polygonum cuspidatum*. *Macromolecular Res* 14:324–330
12. Maron DJ (2004) Flavonoids for reduction of atherosclerotic risk. *Curr Atheroscler Rep* 6:73–78
13. Baur JA, Sinclair DA (2006) Therapeutic potential of resveratrol: the in vivo evidence. *Nat Rev Drug Discov* 5:493–506
14. Das S, Tosaki A, Bagchi D, Maulik N, Das DK (2006) Potentiation of a survival signal in the ischemic heart by resveratrol through p38 mitogen-activated protein kinase/mitogen- and stress-activated protein kinase 1/cAMP response element-binding protein signaling. *J Pharmacol Exp Ther* 317:980–988
15. Fukuda S, Kaga S, Zhan L, Bagchi D, Das DK, Bertelli A (2006) Resveratrol ameliorates myocardial damage by inducing vascular endothelial growth factor angiogenesis and tyrosine kinase receptor Flk-1. *Cell Biochem Biophys* 44:43–49
16. Raval AP, Dave KR, Perez-Pinzon MA (2006) Resveratrol mimics ischemic preconditioning in the brain. *J Cereb Blood Flow Metab* 26:1141–1147
17. Kumar A, Kaundal RK, Iyer S, Sharma SS (2007) Effects of resveratrol on nerve functions, oxidative stress and DNA fragmentation in experimental diabetic neuropathy. *Life Sci* 80:1236–1244
18. Tachiya M (1982) Kinetics of quenching of luminescent probes in micellar systems II. *J Chem Phys* 76:340–348
19. Horrocks WD, Collier WE (1981) Lanthanide ion luminescence probes. Measurement of distance between intrinsic protein fluorophores and bound metal ions: quantitation of energy transfer between tryptophan and terbium(III) or europium(III) in the calcium-binding protein parvalbumin. *J Am Chem Soc* 103:2856–2862
20. Förster T (1965) In: Sinanoglu O (ed) *Modern quantum chemistry*. vol. 3. Academic, New York, pp 93–137
21. Wang C, Wu QH, Wang Z, Zhao J (2006) Study of the interaction of carbamazepine with bovine serum albumin by fluorescence quenching method. *Anal Sci* 22:435–438
22. Ross PD, Subramanian S (1981) Thermodynamics of protein association reaction: forces contribution to stability. *Biochemistry* 20:3096–3102
23. Timaseff SN (1972) *Proteins of biological fluids*. Pergamon, Oxford, pp 511–519, 45
24. Liu ZD, Huang CZ, Li YF, Long YF (2006) Enhanced plasmon resonance light scattering signals of colloidal gold resulted from its interactions with organic small molecules using captopril as an example. *Anal Chim Acta* 577:244–249
25. Xiao JB, Yang CS, Ren FL, Jiang XY, Xu M (2007) Rapid determination of ciprofloxacin lactate in drugs by Rayleigh light scattering technique. *Meas Sci Technol* 18:859–866
26. Xiao JB, Chen JW, Ren FL, Yang CS, Xu M (2007) Use of 3-(4,5-dimethylthiazol-2-yl)-2,5-diphenyl tetrazolium bromide for rapid detection of methicillin-resistant *Staphylococcus aureus* by resonance light scattering. *Anal Chim Acta* 589:186–191
27. Chen JW, Yang CS, Ren FL, Xiao JB, Xu M (2007) Highly sensitive determination of chloride ion in serum using Rayleigh light scattering technique. *Meas Sci Technol* 18:2043–2047
28. Chen ZG, Liu JB, Han YL, Zhu L (2006) A novel histidine assay using tetraphenylporphyrin manganese (III) chloride as a molecular recognition probe by resonance light scattering technique. *Anal Chim Acta* 570:109–115